# Two-electron transfer reactions involving three paraboloidal potential surfaces in solvents with multiple solvation time scales

T. Bandyopadhyay, Akira Okada, and M. Tachiya

Citation: The Journal of Chemical Physics **110**, 9630 (1999); doi: 10.1063/1.478951
View online: http://dx.doi.org/10.1063/1.478951
View Table of Contents: http://scitation.aip.org/content/aip/journal/jcp/110/19?ver=pdfcov
Published by the AIP Publishing

# Two-electron transfer reactions involving three paraboloidal potential surfaces in solvents with multiple solvation time scales

T. Bandyopadhyay,[a] Akira Okada, and M. Tachiya
*Department of Physical Chemistry, National Institute of Materials and Chemical Research, Tsukuba, Ibaraki 305-8565, Japan*

(Received 2 November 1998; accepted 24 February 1999)

The effect of solvent nuclear relaxation dynamics on the rate of two-electron transfer reaction is investigated. We present here a generalized treatment of the Zusman and Beratan model of two-electron transfer reaction using a theoretical scheme that starts from the Liouville equation of motion for the electronic population wave packets to obtain the transfer rates following projection operator formalism. This generalization enables us to treat the three free energy surfaces (three surfaces for $D-A$, $D^{+}-A^{-}$, and $D^{+2}-A^{-2}$ donor–acceptor pairs) involved in such reactions on an equal footing such that the rates for each one- and two-electron transfer step can be obtained when all three diabatic surfaces are present in the system with nonzero electronic coupling elements between them. The reaction takes place on a two-dimensional potential energy surface with two coordinates representing the solvent polarization. The dynamics are governed by overdamped diffusion along these polarization coordinates with different solvent polarization time scales. The resulting equations, that can interpolate the situation between the nonadiabatic and the diffusion limits of electron transfer, are solved numerically for the choice of parameters that validates the criterion for solvent dynamics-influenced rate limit. The transfer rates, in this limit, are found to depend strongly on the multiplicity of the solvent polarization coordinate used. New dynamical solvent effects on the transfer rates in solvents with one or more characteristic relaxation time scales are identified because of the effective participation of all three electronic states in the transfer process. The theoretical recipe developed here is not limited to two-electron transfer problems and can be applied for multiple electron transfer events in solvents with multiple relaxation time scales.
 [S0021-9606(99)51619-X]

## I. INTRODUCTION

Multielectron-transfer events are an important class of reaction in a variety of synthetic, catalytic, fuel cells, optical energy conversion, and biological processes.[1,2] Much of our ability to covert optical energy into chemical energy, by redox mechanism, depends on the multiplicity of electron transferred upon light absorption. The electroreduction of $CO_2$ in aqueous media to prepare fuels or chemicals almost always involves multiple electron-assisted reduction. In fact, the value of one-electron redox potential of $CO_2$ is such that the one-electron reduction process is highly unfavorable.[1(a)] The flavin chromophore of the flavoproteins that take part in many important photobiological processes, can readily undergo both one- and two-electron transfer pathways.[2(a)] These pathways are regulated by the protein part of the enzyme. A specific electronic structure of the flavin chromophore can cause it to accept an electron pair by two channels, either by a sequential uptake of two electrons in two different redox steps or by a concerted process, when the electron pair from the reducing substrate is transferred to the flavin molecule in a single step. Cytochrome *c* peroxidase compound that catalyzes the reduction of hydrogen peroxide to water by cyctochrome *c* and is used extensively to understand biological electron transfer reactions has recently been found to involve a two-electron redox mechanism.[2(c)]

To deal with such systems, one is first posed with the question whether the transfers occurs sequentially[2(a)] or in a concerted manner. If sequentially, then the rates of each transfer steps need not be identical because the driving force of each monoelectron transfer event might not be the same. Only recently, kinetic discrimination between the one-electron processes of a two-electron transfer process has been observed by Pierce and Geiger[2(b)] through the electrochemical method. It should be mentioned that electrochemical experiments occur on rather slow time scales and therefore one could easily misinterpret the underlying microscopic mechanism (sequential or concerted) of the electron transfer (ET) reaction. True multielectron charge transfer processes are not known in the realm of conventional photochemistry. And, to our knowledge, no ultrafast time-resolved studies have been carried out for such multiple charge transfer events in liquid solution. However, one can design molecules that can be utilized to mimic photon-induced multielectron charge transfer;[2(c)] quantum yield of this process depends much on the solvent used. On the other hand, proton transfer coupled with multielectron transfer that can be studied in the realm of photochemistry is also well known.[2(d),(g)] Of course, the mechanism of these electron

[a]On leave from: Chemistry Division, Bhabha Atomic Research Center, Trombay, Mumbai 400 085, India.

 

transfer reactions depend on the *p*H of the solution that has been used to carry out such experiments.

In view of the importance of understanding the mechanism and associated kinetics of this system, it is surprising that only a very few theoretical attempts[3–5] have been made in this direction. The majority of theoretical studies on ET reactions considers only a monoelectron shift from donor to acceptor. The theoretical approach as proposed by Marcus[6] and Levich[7] has witnessed much success and utility during the last four decades. These theories are indeed equilibrium (golden rule approach) theories of ET reaction rates where the solvent polarization is in equilibrium with the momentary charge distribution between the donor and the acceptor pair. These theories have been extended to include the effects due to the influence of solvent dynamics, as there are occasions when the equilibrium assumption no longer holds true.[8–15] Roy and Bagchi[16(a)] have presented a time-dependent solution of the Zusman kinetics that can be applied to various experimental situations. Quite recently, Barbara *et al.* have given a complete account of this single ET reaction in an excellent review article.[16(b)] Of course, there are important classes of reactions, as mentioned above, that involve more than one electron being transferred. Until quite recently,[4] the level of theory for such processes has lagged behind in comparison to standard ET theories which deal with only one-electron transfer processes. Multiple ET theory will evidently be more complex than that for mono ET, as it is intrinsically a three-state system consisting of ground-state donor–acceptor (state 1: $D-A$), singly reduced acceptor and singly oxidized donor (state 2: $D^{+}-A^{-}$), and its doubly redox counterpart (state 3: $D^{+2}-A^{-2}$). ET rates in the presence of multiple sinks in a multisurface problem are found not to be additive.[16(a),(c)] Rather, an interesting nonlinear effect on the ET rates are found due to the presence of multiple sinks,[16(a)] more so in the case of a non-Debye solvent with multiple relaxation timescales.[16(c)] Similar to this, in a two-ET process ground-state donor–acceptor pair are connected with two charge transfer states, $D^{+}-A^{-}$ and $D^{+2}-A^{-2}$, and evidently such a nonlinear effect is expected to be present. In addition to this, the present situation that we consider in this work is more complex because of the fact that the two charge-transfer states are also connected with each other, allowing the sequential transfer from state 1 to state 3 via the intervening and intermediate state 2. Our generalization of the Marcus equation for ET rate[17] can be readily recast into multiple ET events to obtain their rates when equilibrium thermal distribution of population over reaction coordinate is assumed.[18]

In order to account for the dynamical solvent effects in the multiple ET processes, Zusman and Beratan (ZB)[4,5] considered two-ET reactions in a polar solvent with Debye characteristics. In other words, a single solvation coordinate is chosen by projecting the fluctuating bath degrees of freedom onto a one-dimensional coordinate system. This is indeed a single collective solvation coordinate, since it represents the multidimensional potential energy surfaces constructed by the bath degrees of freedom where the reaction is thought to take place. Thus, a Zusman strategy[8(a)] was adapted in Refs. 4 and 5 to obtain the competitive rates of transfer for the unconventional sequential mechanism where the reaction intermediates are not separated diffusionally, and for that of the concerted mechanism. As two-ET reactions combine aspects of both sequential and concerted transfer, and since these two channels of transfer are difficult to distinguish experimentally, it is useful to consider the qualitative differences between them. (Although such a possibility of discrimination has only began to appear recently by electrochemical method[2(b)].) The reaction scheme that we have studied here is similar to that of ZB:[4,5]

$$D+A\Leftrightarrow(D\cdots A)\Leftrightarrow(D^{+}\cdots A^{-})\Leftrightarrow(D^{+2}\cdots A^{-2})\Leftrightarrow D^{+2}+A^{-2}\ (\text{stepwise}) \tag{1a}$$

$$D+A\Leftrightarrow(D\cdots A)\Leftrightarrow(D^{+2}\cdots A^{-2})\Leftrightarrow D^{+2}+A^{-2}\ (\text{concerted}). \tag{1b}$$

In the unconventional stepwise mechanism [Eq. (1a)], the two electrons are transferred sequentially in a single collision complex before the one-electron donor–acceptor intermediate can be separated in the reaction volume by diffusion. Thus, the stepwise transfer mechanism that we consider here proceeds without a detectable concentration of the one-electron intermediates. The electronic coupling elements between the donor–acceptor pairs in the two steps of transfer may or may not be equal. In contrast, in a concerted mechanism [Eq. (1b)] the two electrons are transferred in a single step with an electronic coupling that can be assumed to be much smaller than that of the sequential steps.

However, in order to obtain the elegant expressions for the stepwise ET rates, ZB[4,5] have considered that the electronic coupling element between the donor–acceptor states, 1 and 3 are zero. Similarly, to obtain the concerted rates, ZB have equated the problem with the corresponding two-state problem. That is, the intermediate donor–acceptor electronic state is absent while calculating the concerted ET rate in the ZB approach.[4,5] On the other hand, one naively expects all three electronic states to be present with nonzero electronic coupling elements between them such that the concerted and sequential transfer rates might influence each other. In view of this, one of the principal objectives of the present study is to extend the ZB model[4] of two-ET reaction so that all three electronic states participating in the reaction are present in the system with nonzero electronic coupling between them. Such a consideration is important and might have far-reaching consequences (new solvent dynamic effects) as we shall present below. As already mentioned above, the basic impetus of such a consideration is the fact that transfer rate to a particular sink is strongly correlated with the presence of the other.[16(a),(c)]

One of the basic assumptions in ZB's approach[4] of two-ET reactions directly follows from Zusman's strategy for single-electron ET reactions.[8(a)] Namely, the assumption of high activation barriers (compared to thermal energies) both for the transfer steps from surface 1 to 2 and also for the concerted step from 1 to 3. This condition can be achieved by either changing the free-energy difference between the surfaces or by increasing the solvent reorganization energies. For example, for the sequential step $1\rightarrow 2$ one assumes

$\Delta G_{21} > k_B T$, which is physically justifiable by the fact that surface 2 is unstable with respect to surface 1 such that the reaction proceeds without any detectable concentration of the intermediate electronic state. On the other hand, for the concerted process, since the solvent reorganization energy scales with the square of the charge transferred and since for a polar solvent the reorganization energy associated with single ET is typically ~1 ev—this reorganization energy might offer a mechanism against the high activation barrier assumption (depending on the values of $\Delta G_{13}$). Nevertheless, the concerted process in principle can occur as in the single-ET process in a wide range of activation energies—normal, barrierless, and in the inverted regime. The basic advantage behind the assumption of a high activation barrier is that the long-time transfer kinetics is exponential such that the thermal equilibrium of the population wave packet in the initial surface is maintained. The transfer rate thus becomes independent of the ''initial position'' of the population wave packets along the polarization potential surfaces. However, as we shall present below, because of the effective participation of all three surfaces, the transfer kinetics between two surfaces will eventually be comprised of a contribution from thermal equilibrium population of the wave packets and from contributions of wave packets before being thermalized. Note that the other possibility of sequential thermalization followed by ET for an initially localized wave packet has previously been considered by Rips and Jortner in the context of activationless single-ET reaction.[11(c)]

As stated above, for a polar solvent, since the solvent reorganization can be high especially for the concerted process, this can be much greater than the physically acceptable values of electronic coupling strength. This reduces the adiabaticity of the concerted transfer reaction. On the contrary, to obtain a diffusion-influenced limit the electronic coupling strength should be high or else the solvent relaxation rate should be sufficiently slow. Therefore, there must be a tradeoff between these ET parameters such that the transfer rate effectively couples with solvent relaxation. This is also discussed at length in this work.

The influence of solvent dynamics on the single-ET reactions[8–15,19] is rather a well-studied class of reactions. The studies have offered a unique view of chemical dynamics in solution and have established extensive close relationships between ultrafast ET experiments, molecular level and approximate theories, and molecular level simulations.[16(b)] The studies under this category include solvents whose relaxation dynamics in the presence of a solute can be described by a single relaxation time (Debye solvent), as well as solvents such as alcohol and other hydrogen-bonding solvents that exhibit multiple relaxation time scales (non-Debye solvent). Recent ultrafast ET studies[20] have revealed the role of complex solvent and solute nuclear relaxation motion dynamics on the ET rates. These suggest that the assumption of a solvent with single relaxation time is not sufficient to support the multiple relaxation time phenomenon. To this end, theory of ET reactions in solvents with two characteristic relaxation time was developed by Zusman.[8(c)] Zusman's approach[8(a)] was also used to include the solvents with arbitrary spectral density (a quantity that contains all the information regarding nuclear properties which influence electronic motion) using a single solvation coordinate and a time-dependent kernel.[13] More recently, a microscopic theory of ET rates in solvents with complex spectral densities has been developed[19] using a multiple solvent coordinate system which were identified as a nuclear collective mode. A clear difference of the usage of two collective solvent coordinates on the ET rates is obtained in comparison to the traditional use of one reaction coordinate when all other solvent motions are thought to undergo fast relaxation (and does not affect the ET rate).[19] The nuclear collective coordinates can be classified into two categories: the primary one that couples directly with the ET dynamics, and the secondary one that couples with the primary nuclear coordinates and can be treated as a hidden coordinate of the solvent bath. A merit of this approach is the fact that the number of collective solvent coordinates to be used directly follows from the experimentally measured quantities such as solvent spectral densities or the time-correlation function of the solvation energy of the reacting system. As already mentioned, the rate of ET from a locally excited electronic state in the presence of multiple sinks can exhibit extreme values, especially in a non-Debye solvent[16(c)] such as *n*-propanol (in comparison to that in a solvent with single average relaxation time).[16(a)] Therefore, it would be interesting to investigate such solvent effects pertaining to the kinetics of outer-sphere two-ET reaction involving three surfaces where each of these surfaces are connected to two sinks.

Following this, the purpose and scope of the present work is to present microscopic theory for multi-ET events between the donor and acceptor pair embedded in a solvent with multiple relaxation time scales such that all the possible donor–acceptor electronic states are participating in the transfer process with nonzero electronic coupling elements between them. However, the results will be presented for experimentally interesting phenomenon of two-ET in a solvent with two characteristic relaxation time scales. It is to be noted that the results obtained in Ref. 19 cannot be used for numerical calculation (in the long-time limit), except for the two electronic surface cases, because of a divergent term. Therefore, that formulation cannot be used as such for the two-ET problem, which is intrinsically a three-surface problem. We would also like to point out at this stage that when the solvent can be represented by a single relaxation time scale, our general approach reduces to that of ZB, with one basic difference being the presence of all the electronic states together with nonzero electronic couplings between them.

Our approach in this work is as follows. In Sec. II we present the basic theoretical formulation to treat such a system where there are many electronic states coupled to many nuclear modes. There, the expression for ET rates is derived following a projection operator formalism. Application of the present formulation for two-ET reaction in solvents which has two solvation time scales is made in Sec. III in the long-time limit. There, we present the numerical results for several choices of transfer parameters that validate the criterion for solvent dynamics-influenced rate limit and also compare with the results obtained using a Debye solvent. At the

end, the main conclusions of the proposed treatment are summarized.

## II. MULTISURFACE ET REACTION IN SOLVENTS WITH MANY RELAXATION TIMES

The principal aim of this work is to study the two-ET reactions involving three Marcus-type paraboloidal surfaces in a two-dimensional solvent coordinate system, such as in a three-component system involving a reactant ($D-A$; 1st electronic state), an intermediate ($D^+-A^-$; 2nd electronic state), and the final product ($D^{+2}-A^{-2}$; 3rd electronic state) that follows from Eq. (1). The particles in this three-component system are surrounded by polar solvent molecules. The solvent polarization dynamics in all the coordinates are thought to be in the high-friction overdamped diffusion limit. Therefore, the solvent relaxation can be characterized in terms of a finite number of exponentials along these coordinates. With such an assumption, the stochastic Liouville equation of Zusman[8(a)] for the electronic population wave packets $\rho_{mm}(\mathbf{q},t)$ and the corresponding Liouvillian operator can be written as

$$\frac{d}{dt}\rho_{mm}(\mathbf{q},t)=-iL_m^{(0)}\left(\mathbf{q},\frac{\partial}{\partial\mathbf{q}}\right)\rho_{mm}(\mathbf{q},t)+\sum_{m'}k_{mm'}(\mathbf{q})\rho_{mm'}(\mathbf{q},t), \tag{2}$$

where

$$L_m^{(0)}\left(\mathbf{q},\frac{\partial}{\partial\mathbf{q}}\right)\equiv i\sum_{\alpha=1}^{N}\frac{\Lambda_\alpha}{2}\frac{\partial}{\partial q_\alpha}\left[\frac{\partial U_m(\mathbf{q})}{\partial q_\alpha}+k_{\mathrm{B}}T\frac{\partial}{\partial q_\alpha}\right], \tag{3}$$

$$k_{mm'}(\mathbf{q})\equiv\frac{2\pi}{\hbar}|V_{mm'}|^2\delta[U_m(\mathbf{q})-U_{m'}(\mathbf{q})]\quad(\text{for } m\neq m'), \tag{4}$$

$$k_{mm}(\mathbf{q})\equiv-\sum_{m'(m'\neq m)}k_{m'm}(\mathbf{q}), \tag{5}$$

and

$$U_m(\mathbf{q})\equiv\sum_{\alpha=1}^{N}[(q_\alpha-d_{\alpha,m})^2-d_{\alpha,m}^2]+E_m. \tag{6}$$

In these expressions, $\mathbf{q}$ is the coordinate operator. $\mathbf{q}$ can be thought of as representing the set of collective coordinates including the effects of all nuclear degrees of freedom on the motion of electronic population wave packets. In the solvent dynamics-controlled limit, the operator $\mathbf{q}$ entails the dynamics of dielectric fluctuations in the solvent bath on the ET rate. Favorable fluctuations that make the initial and final states isoenergetic induce the transfer. The number of collective coordinates finally required to calculate a particular observable of interest directly follows from experiments, instead of the usual initial guess of an arbitrary number of solvent coordinates.[19] Equation (3) designates a sum of standard Smoluchowski diffusion operators for $N$ high friction and overdamped collective nuclear diffusive modes $\alpha$, and the diffusion occurs within the free-energy paraboloid of each of the electronic states, $m$. The dynamics of wave packets along each coordinate $q_\alpha$ is characterized by a relaxation rate $\Lambda_\alpha$ and the temperature $T$. $k_{\mathrm{B}}$ is the Boltzmann constant. The free-energy paraboloids are given by Eq. (6). In Eq. (6), $d_{\alpha,m}$ denotes the displacement of the $\alpha$th oscillator by populating the $m$th electronic state that has an energy equal to $E_m$ without the solvation effects. The second term on the right-hand side of Eq. (2) can be broken into two separate terms representing the source and sink function that changes the population of the $m$th electronic state by reaction through the electronic coupling elements, $|V_{mm'}|$ between the surfaces $m$ and $m'$. In other words, the ET reaction considered here is reversible and the sink for forward transfer from a given electronic state also serves as source for back transfer, although throughout the text we have used the generic term ''sink'' to represent a reversible process. The $\delta$ function term in Eq. (4) is the $\mathbf{q}$-set of collective coordinate dependent sink functions which specifies the position and therefore the energy of the free-energy surface at which the electron transfer takes place between the surfaces $m$ and $m'$. We will refer to this curve crossing region between the reactant and the product surfaces as the exit channels or transition space. Equation (4) also implies that the Franck–Condon principle is implicitly built into Eq. (2).

The equation of motion [Eq. (2)] is written based on two assumptions—one is the assumption of separability of nuclear motion from electronic motion and the other is the absence of quantum effect of nuclear motion. This equation has several alluring features. First, it is a reaction-diffusion equation [when the operator $L_m^{(0)}(\mathbf{q},\partial/\partial\mathbf{q})$ is viewed as a Smoluchowski-type diffusion operator in the high-friction limit] that describes the dynamics of many electronic states coupled to many nuclear degrees of freedom, and being a differential equation is rather easy to handle. Second, for multiple ET in solvents with many relaxation time scales, this is just what we desire to have in order to explain the dynamics of ET when $U_m(\mathbf{q})$ represents a free-energy paraboloidal well. In addition to this, the above equation holds true both in the nonadiabatic and the diffusion limits of ET as well as in the intermediate limits. Third, since it is a classical equation of motion in the $(\mathbf{q},t)$ phase space, all the quantities that appear in this equation are physically observable. In view of these features and our principal objective here, we will utilize this equation of motion to obtain the formal ET rates for many electronic states in a bath with many nuclear modes.

The form of the potential surface $U_m(\mathbf{q})$ in the $N$-dimensional space characterizes polarization fluctuations caused by the $N$ primary oscillators of the solvent bath. The motion along the $N$-dimensional surface leads to reaction at a sink located in some region on the surface. For a reversible reaction, motion along both the reactant and the product surfaces are relevant. Equation (6) also signifies that the polarization potential energy surface is a sum of $N$ noninteracting potential surfaces. Thus, motion along the $q_\alpha$ coordinates is separable. This is a major assumption necessary for solving the equation of motion [cf. Eq. (2)] by Green's function technique. However, this simplest model should reflect the significant qualitative features of the multidimensional processes.

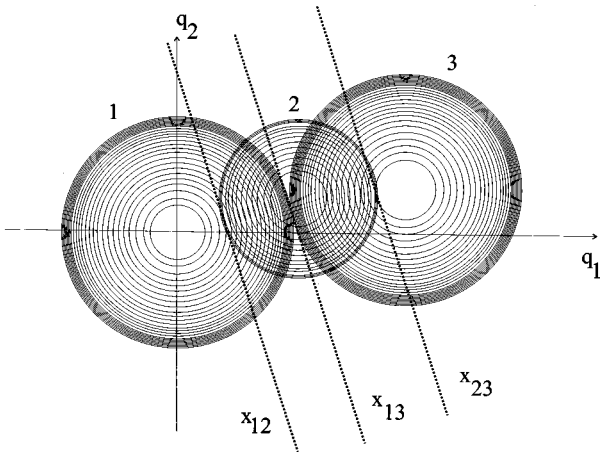


FIG. 1. Schematic contour plots of the potential energy surfaces for two-ET reaction in two collective solvent coordinates, $\mathbf{q}_1$ and $\mathbf{q}_2$. The transfer is thought to take place along the sink line $x_{mm'}$. 1, 2, and 3 represent the three surfaces associated with this reaction.

As an example of the two-dimensional case, in Fig. 1 we draw contour plots of three harmonic wells associated with the three donor–acceptor redox states. The coordinates $q_1$ and $q_2$ in this figure denote two collective nuclear degrees of freedom associated with the electron transfer between donor and acceptor states. In this two-coordinate system, the sink function $k_{mm'}(q_1,q_2)$ signifies a line of sink density, $x_{mm'}$ (see below for definition) in Fig. 1. Therefore, the leakage of electronic population wave packets from one surface to the other occurs along this line of sink density. In Sec. III we will expand on this picture to serve as a model for the two-ET problem influenced by solvent relaxation along the two collective coordinates.

A reorganization energy of the collective coordinate $\alpha$, which denotes the strength of coupling between solvent bath along the coordinate $q_\alpha$ and the electronic state, and total reorganization energy for the transition between the two electronic states, are denoted by $\lambda_{\alpha,mm'}$ and $\lambda_{mm'}$, respectively. They are given by

$$\lambda_{\alpha,mm'}=(d_{\alpha,m}-d_{\alpha,m'})^2, \tag{7}$$

$$\lambda_{mm'}=\sum_{\alpha=1}^{N}\lambda_{\alpha,mm'}. \tag{8}$$

Let us denote the free-energy gap between the surfaces and a reaction (or solvation) coordinate for the transition between the $m'$ and $m$th electronic states by $\Delta G_{mm'}$ and $\Delta Z_{mm'}(\mathbf{q})$, respectively. They are given as

$$\Delta G_{mm'}=G_m-G_{m'}=-\sum_{\alpha=1}^{N}d_{\alpha,m}^2+E_m+\sum_{\alpha=1}^{N}d_{\alpha,m'}^2-E_{m'}, \tag{9}$$

$$\Delta Z_{mm'}(\mathbf{q})=-2\sum_{\alpha=1}^{N}(d_{\alpha,m}-d_{\alpha,m'})q_\alpha. \tag{10}$$

The reason behind such a choice of reaction coordinates directly follows from Eq. (4). That is, in order for the transition between two electronic states to take place, the free-energy wells must equate with each other, $U_m(\mathbf{q})=U_{m'}(\mathbf{q})$, such that the transfer can take place only at nuclear configurations where the reaction coordinates have certain specified values;

$$\Delta Z_{mm'}(\mathbf{q})=-E_{mm'}=-(E_m-E_{m'}). \tag{11}$$

Earlier, we called this space of nuclear configuration exit channels or a transition space. We now define coordinate $x_{mn}$ to specify a point on this line in a system of solvent with two collective coordinates as,

$$\begin{pmatrix}q_1(x_{mn})\\ q_2(x_{mn})\end{pmatrix}\equiv\frac{1}{\sqrt{\lambda_{mn}}}\begin{pmatrix}-(d_{2m}-d_{2n})\\ (d_{1m}-d_{1n})\end{pmatrix}x_{mn}+\frac{1}{\sqrt{\lambda_{mn}}}\begin{pmatrix}-(d_{1m}-d_{1n})\\ (d_{2m}-d_{2n})\end{pmatrix}y_{mn}+\begin{pmatrix}d_{1n}\\ d_{2n}\end{pmatrix}, \tag{12}$$

with

$$y_{mn}\equiv-\frac{1}{\sqrt{\lambda_{mn}}}\left[(d_{1m}-d_{1n})d_{1n}+(d_{2m}-d_{2n})d_{2n}-\frac{E_m-E_n}{2}\right]. \tag{13}$$

Thus, as stated above, $x_{mm'}$ represents a line of sink through which transfer of population between two electronic states can take place. In Laplace space, the generalized ET rate matrix, $\mathbf{K}(s)$, for this system is defined by the projection operator formalism and is given by[21]

$$s\mathbf{P}(s)-\mathbf{1}=\mathbf{K}(s)\mathbf{P}(s), \tag{14}$$

where $\mathbf{1}$ is a unit matrix, and $\mathbf{P}(s)$ is a matrix whose elements $P_{ml}(s)$ are populations of the $m$th electronic state with the $l$th initial condition taken such that $[\rho(\mathbf{q},t=0)]_m=\delta_{ml}\overline{\rho_l}(\mathbf{q})$. Here, the equilibrium distribution for the $l$th electronic state, $\overline{\rho_l}(\mathbf{q})$ is $e^{-\beta U_l(\mathbf{q})}/\int d\mathbf{q}'\,e^{-\beta U_l(\mathbf{q}')}$ ($\beta=1/k_BT$). For an $N$ coordinate system, this is given by

$$\overline{\rho_l}\equiv\prod_\alpha\frac{1}{\sqrt{\pi k_BT}}\exp\left[-\frac{1}{k_BT}(q_\alpha-d_{\alpha,l})^2\right]. \tag{15}$$

The Laplace transform of $f(t)$ in Eq. (14) has been denoted by $f(s)$

$$\left(f(s)\equiv\int_0^\infty dt\,e^{-st}f(t)\right).$$

It can be shown using Eq. (14)[21] that

$$\Sigma_{m'}K_{m'm}(s)=0, \tag{16}$$

and that the detailed balance condition,

$$K_{m'm}(s)e^{-\beta G_m}=K_{mm'}(s)e^{-\beta G_{m'}}, \tag{17}$$

holds for the transfer rates. Using Eqs. (2)–(6) and Eq. (14), it can be shown[21] that the Laplace-transformed ET rate for transfer from $m \rightarrow m'$ levels is given by

$$K_{m'm}(s) \equiv \langle m' | \hat{V} \hat{h}^{-1}(s) | \overline{\rho}_m \rangle, \tag{18}$$

where the operator $\hat{h}$ is defined as

$$\hat{h}(s) \equiv 1 + \hat{g}(s)\hat{V}, \tag{19}$$

and the matrix elements for the operator $\hat{g}(s)$ are given by

$$g_m(\mathbf{q}, \mathbf{q}'; s) \equiv \int dt\, e^{-st} [\mathcal{G}_m(\mathbf{q}, \mathbf{q}'; t) - \overline{\rho}_m(\mathbf{q})]. \tag{20}$$

Equation (20) gives the Laplace-transformed conditional probability for the solvation coordinate after eliminating the divergent term in the long-time limit, as was mentioned in the introduction. Its time analog, $g_m(\mathbf{q}, \mathbf{q}', t)$, represents the same conditional probability to have the value $\mathbf{q}$ given that it had a value $\mathbf{q}'$ at time $t=0$ on a multidimensional surface. A Green's function for the Smoluchowski operator $L_m^{(0)}$ is given as

$$\mathcal{G}_m(\mathbf{q}, \mathbf{q}'; t) \equiv \prod_\alpha \frac{1}{\sqrt{2\pi\sigma_\alpha(t)}} \exp\left\{ -\frac{1}{\sqrt{2\sigma_\alpha(t)}} \times [(q_\alpha - d_{\alpha,m}) - (q'_\alpha - d_{\alpha,m}) M_\alpha(t)]^2 \right\}, \tag{21}$$

with

$$\sigma_\alpha(t) \equiv \frac{k_B T}{2} \{1 - [M_\alpha(t)]^2\}; \tag{22}$$

and

$$M_\alpha(t) \equiv \exp(-\Lambda_\alpha t). \tag{23}$$

In Eq. (18), the inner product with $\langle m|$ is described by

$$\langle m | f \rangle \equiv \sum_n \int d\mathbf{x}_{mn}\, f_{mn}(\mathbf{x}_{mn}). \tag{24}$$

In the present framework, the solvent dynamics is contained in the expression for $M_\alpha(t)$ (which finally appears in the operator $\hat{h}$), where $\Lambda_\alpha^{-1}$ represents the relaxation time scale along the collective solvent coordinate $\alpha$. The expression for the ET rate, [Eq. (18)] is the key equation for numerical calculation of the rates and can be seen to accomplish the following properties for ET rates in solution. (1) It holds for nonadiabatic and solvent dynamic control range of transfer, as well as in any intermediate electronic coupling strengths. Using this expression, when we consider lowest-order contribution of $V$ based on nonadiabatic perturbation theory, which is called the golden rule limit, we have

$$k_{mm}^{(\mathrm{non})} = \frac{2\pi |V_{m'm}|^2}{\sqrt{4\pi \lambda_{m'm} k_B T}} \times \exp\left[ -\frac{(\Delta G_{m'm} + \lambda_{m'm})^2}{4\lambda_{m'm} k_B T} \right] \quad \text{for} \quad m' \neq m, \tag{25}$$

(2) In the diffusion limit when solvent polarization dynamics is very slow as compared to transfer rate, i.e., the reaction adiabaticity is very high, we can replace $Vh^{-1}(s)$ by $g^{-1}(s)$ to obtain the solvent dynamics controlled (adiabatic) rate from Eq. (18),

$$k_{m'm}^{(\mathrm{dif})} = \langle m' | \hat{g}^{-1}(s) | \overline{\rho}_m \rangle. \tag{26}$$

In this case, the intensity of the sink function is so large that the motion inside the potential well determines the reaction rate. (3) In the intermediate coupling regime where the ET rate and the solvent polarization dynamics couple with each other effectively, a solvent with sufficiently slow relaxation time scale will add to the dominance of the adiabatic contribution to the ET dynamics.

For the sake of numerical calculation, we further recast the elements of the rate matrix [cf. Eq. (18)] into the following form:

$$\begin{aligned} k_{mm'}(s) = \sum_{n'} \int dx'_{n'(n'+1)} \sum_n \int dx_{n(n+1)} & \times (\delta_{m'n'} - \delta_{m'(n'+1)}) \frac{\pi |V_{n'(n'+1)}|^2}{\hbar \sqrt{\lambda_{n'(n'+1)}}} \\ & \times h^{-1}(n'(n'+1), x'_{n'(n'+1)}; n(n+1), x_{n(n+1)}, s) \\ & \times (\delta_{(n+1)m} - \delta_{nm}) \overline{\rho}_m(x_{n(n+1)}). \end{aligned} \tag{27}$$

In this expression, $h^{-1}$ is an inverse of $h$ such that

$$\begin{aligned} & \delta_{n''n} \delta(x''_{n''(n''+1)} - x_{n(n+1)}) \\ & \equiv \sum_{n'} \int dx'_{n'(n'+1)} h(n''(n''+1), x''_{n''(n''+1)}; \\ & \quad n'(n'+1), x'_{n'(n'+1)}, s) h^{-1}(n'(n'+1), \\ & \quad x'_{n'(n'+1)}; n(n+1), x_{n(n+1)}, s), \end{aligned}$$

and the elements of $\hat{h}$ are calculated as

$$\begin{aligned} & h(n'(n'+1), x'_{n'(n'+1)}; n(n+1), x_{n(n+1)}, s) \\ & \equiv \delta_{n'n} \delta(x'_{n'(n'+1)} - x_{n(n+1)}) + \begin{bmatrix} \delta_{n'n} g_n(x'_{n'(n'+1)}, x_{n(n+1)}, s) + \delta_{n'n} g_{n+1}(x'_{n'(n'+1)}, x_{n(n+1)}, s) \\ - \delta_{n'(n+1)} g_{n+1}(x'_{n'(n'+1)}, x_{n(n+1)}, s) - \delta_{(n'+1)n} g_n(x'_{n'(n'+1)}, x_{n(n+1)}, s) \end{bmatrix} \frac{\pi |V_{n(n+1)}|^2}{\hbar \sqrt{\lambda_{n(n+1)}}}. \end{aligned} \tag{28}$$

Here, $g_m(\mathbf{q}',\mathbf{q},s)$ can be obtained from Eq. (20) and $g_n(x'_{n'(n'+1)},x_{n(n+1)};s)$ is defined as $g_n(\mathbf{q}'(x'_{n'(n'+1)}),\mathbf{q}(x_{n(n+1)});s)$, which is calculated by substituting Eqs. (12) and (13) into Eq. (20). The Green function for Smoluchowski operator is given by Eqs. (21)–(23) and for solvent with two relaxation time scales we use $\alpha=2$.

The ET rates obtained following this recipe differ in many aspects when compared with the ZB approach.[4] First, the ET rates in the present formalism can describe solvents with multiple relaxation time scales, in contrast to ZBs formalism with solvent having Debye characteristics. Second, in contrast to ZBs approach the present formalism applies to any arrangement of free-energy wells (1 and 3) such that the concerted reaction rate can be obtained in normal, activationless as well as in the inverted regime. For example, ZBs expression for concerted two-ET rate in the adiabatic limit is not applicable to low barrier reactions. Third, in the present formalism the sequential and the concerted ET rates can be obtained in the presence of all three diabatic surfaces with nonzero electronic coupling elements between them. Their mutual influence on the ET rate at a given crossing point is contained in the rate matrix elements given in Eq. (27). The sequential rates were obtained by ZB assuming that the electronic coupling between surfaces 1 and 3, $V_{13}$, is zero. Similarly, the concerted two-ET rates were obtained by these authors when the second intermediate surface is assumed to be absent ($V_{12}=V_{23}=0$). As we shall present below, such a consideration of separability of ET rates is inadequate, especially when the sequential and concerted rates are competitive.

Note that when one of the collective coordinates is taken to represent fast intramolecular ligand vibration, the other represents the same solvent polarization dynamics, the reaction sink has a finite width rather than being a delta function, and the reverse reaction is supposed to be absent—our formalism becomes mathematically equivalent to the Sumi–Marcus theory of ET reaction.[15]

In the following section, we will present the results of numerical calculations of the long time ($s=0$) two-ET rates using the formalism developed earlier in this work. Namely, we will consider two-electron transfer reactions in a solvent with two characteristic relaxation times, i.e., with two collective coordinates (cf. Fig. 1). As stated above, due to the $\delta$-function nature of the sink function in Eq. (4), the transfer takes place only along the thin line of sink density, $\mathbf{x}_{mm'}$, in this two-solvent coordinate system. At this stage, in order to appreciate the results of the numerical calculations it will be useful to consider the free energies of the surfaces taking part in the reaction, and the ET rates in a solvent with Debye characteristics.

### A. Free energies of the surfaces

The free energy of the $n$th electronic state as a function of the reaction coordinate, $\Delta Z_{mm'}$, is defined as

$$F_n(\Delta Z_{mm'}) \equiv -k_B T \ln \int d\mathbf{q}\,\delta(\Delta Z_{mm'}(\mathbf{q})-\Delta Z_{mm'}) \times \exp\left(-\frac{U_n(\mathbf{q})}{k_B T}\right), \tag{29}$$

$$= \frac{1}{4\lambda_{mm'}}\left[\Delta Z_{mm'}+2\sum_{\alpha=1}^{N}(d_{\alpha,m}-d_{\alpha,m'})d_{\alpha,n}\right]^2 + G_n + c_{mm'}. \tag{30}$$

In this expression, the constants, $c_{mm'}$ are given by

$$c_{mm'} \equiv \left(\frac{k_B T}{2}\right)\ln\left[\frac{4\pi\lambda_{mm'}k_B T}{(\pi k_B T)^N}\right], \tag{31}$$

With the help of Eqs. (7)–(9) and Eq. (11), Eq. (30) can be recast into the following form for $n=m'$ or $m$:

$$F_n(\Delta Z_{mm'}) = \frac{1}{4\lambda_{mm'}}(\Delta Z_{mm'}+E_{mm'}-\Delta G_{mm'}\mp\lambda_{mm'})^2 + G_n + c_{mm'}, \tag{32}$$

where the negative sign is for $n=m'$ and the positive sign is for $n=m$, that is, to be used in Eq. (30) to obtain this expression. For the two-ET reaction as mentioned above, we have three surfaces corresponding to three redox couples. And, since $d_{\alpha,1}-d_{\alpha,2}=d_{\alpha,2}-d_{\alpha,3}$, one can readily use Eq. (32) to write the following free-energy surfaces for the three states as a function of reaction coordinate $\Delta Z_{12}$:

$$F_1(\Delta Z_{12}) = \frac{1}{4\lambda_{12}}(\Delta Z_{12}+\Delta E_{12}-\Delta G_{12}+\lambda_{12})^2+G_1+c_{12}, \tag{33a}$$

$$F_2(\Delta Z_{12}) = \frac{1}{4\lambda_{12}}(\Delta Z_{12}+\Delta E_{12}-\Delta G_{12}-\lambda_{12})^2+G_2+c_{12}, \tag{33b}$$

$$F_3(\Delta Z_{12}) = \frac{1}{4\lambda_{12}}(\Delta Z_{12}+\Delta E_{23}-\Delta G_{23}-\lambda_{12})^2+G_3+c_{12}. \tag{33c}$$

### B. ET rates for Debye solvent

Here, the two-ET rates are obtained in a Debye solvent which has only one solvation time scale. This physical situation is similar to ZB.[4,5] We start with the rate matrix given by Eq. (14) that includes all the surfaces at any given instant. In Debye solvent, instead of a thin line of sink density (cf. Fig. 1), the reaction here is assumed to be taking place along a single crossing point between any two given free-energy surfaces. In that case, the operator $\hat{h}$ becomes a finite $3\times3$ matrix and the ET rate matrix as given by Eq. (14) with the matrix elements as given by Eq. (18), reduces to

$$\mathbf{K}(s)=\mathbf{IVh}^{-1}(s)\overline{\rho}, \tag{34}$$

where

$$\bar{\rho} \equiv \begin{pmatrix} -\bar{\rho}_1(x_{12}) & \bar{\rho}_2(x_{12}) & 0 \\ 0 & -\bar{\rho}_2(x_{23}) & \bar{\rho}_3(x_{23}) \\ \bar{\rho}_1(x_{31}) & 0 & -\bar{\rho}_3(x_{31}) \end{pmatrix}, \tag{35}$$

$$\mathbf{I} \equiv \begin{pmatrix} 1 & 0 & -1 \\ -1 & 1 & 0 \\ 0 & -1 & 1 \end{pmatrix}, \tag{36}$$

$$\mathbf{h}(s) \equiv \mathbf{1} + \mathbf{g}(s)\mathbf{V}, \tag{37}$$

$$\mathbf{g}(s) \equiv \begin{pmatrix} \Sigma_{m=1,2} g_m(x_{12},x_{12};s) & -g_2(x_{12},x_{23};s) & -g_1(x_{12},x_{31};s) \\ -g_2(x_{23},x_{12};s) & \Sigma_{m=2,3} g_m(x_{23},x_{23};s) & -g_3(x_{23},x_{31};s) \\ -g_1(x_{31},x_{12};s) & -g_3(x_{31},x_{23};s) & \Sigma_{m=3,1} g_m(x_{31},x_{31};s) \end{pmatrix}, \tag{38}$$

and the electronic coupling matrix is given by

$$\mathbf{V} \equiv \begin{pmatrix} \dfrac{\pi |V_{12}|^2}{\hbar \sqrt{\lambda_{12}}} & 0 & 0 \\ 0 & \dfrac{\pi |V_{23}|^2}{\hbar \sqrt{\lambda_{23}}} & 0 \\ 0 & 0 & \dfrac{\pi |V_{13}|^2}{\hbar \sqrt{\lambda_{31}}} \end{pmatrix}. \tag{39}$$

In the above expression, the **g**-matrix elements are given by Eq. (20) with the number of collective nuclear coordinate equal to one and its argument, $x_{mm'}$ that denotes the crossing points between the surfaces is now given by

$$x_{mm'} \equiv \frac{E_m - E_{m'}}{2(d_m - d_{m'})}. \tag{40}$$

It should be noted that in the subsequent work on the solvent dynamic effects on ET rate[11,15] following the pioneering work of Zusman,[8] the relaxation time along the reaction coordinate that determines the value of the diffusion coefficient along this coordinate was taken to be the longitudinal relaxation time. But, as has been shown in Ref. 16(a), this relaxation time should actually be the average solvation time that is obtained from considering all of the polarization modes of the solvent. In our present formulation, since the number of reaction (solvation) coordinates to be used directly follows from the spectral densities of the liquid, and since the latter quantity contains all the information of coupling of the electronic motion to the solvent bath, the solvent relaxation rate that we use here is more microscopic. Therefore, in the present work, a solvent with a single relaxation time, $\Lambda^{-1}$, can be thought to represent the average solvation time, rather than a macroscopic quantity such as the longitudinal relaxation time.

## III. RESULTS AND DISCUSSION

The rate expression, Eq. (27), is rather general and is not limited to two-ET reactions. The solvent dynamics in the present work is contained in the term $M(t)$ and enters the rate expression through the Green's function [Eq. (21)] that could be utilized to obtain the ET rates in a multiple solvent coordinate system. The latter Green's function finally appears in the rate expression through the matrix **h**, as given by Eq. (19) and more explicitly by Eq. (28). Thus, these equations can be utilized to obtain multiple ET rates in solvents with multiple relaxation dynamics. In addition to this, all the diabatic surfaces involved in multiple ET events are assumed to have nonzero electronic coupling between them, such that the transfer rate from a given surface to the other can be calculated in the presence of all other surfaces in the system which can influence each other. In this section, we will calculate the long-time ET rates for two-ET reaction involving three surfaces in solvents with one or more characteristic relaxation time scales.

It follows from the expression for the **h** matrix [Eq. (28)] that when the solvent reorganization energy and the activation barrier is fixed, the reaction adiabaticity is decided by two variables $\Lambda_\alpha$ and $V_{mn}$. If the electronic coupling strength is high and the solvent relaxation rate on the potential surfaces is slow, the effect of the **h** matrix on the transfer rate becomes significant and the transfer rate is controlled by the solvent motion. Any solvent fluctuation that brings the population wave packet to the barrier top becomes crucial in inducing the transfer. We will elaborate below for the choice of parameters to obtain the ET rate in the solvent dynamic control limit. On the other hand, if the electronic coupling is small such that splitting in the mixing region of the two surfaces is small and the solvent relaxation rates are very fast such that equilibrium distribution of population is always maintained, the probability of transfer at the crossing point becomes very low and is rate limiting. The reaction is said to be in the nonadiabatic limit. Under such circumstances, solvent dynamics do not dictate the overall rate and the **h** matrix can be taken to be a unit matrix.

The total ET rate, $k_{31}^{(T)}$ from electronic state 1 to 3 will contain contributions both from sequential steps and from concerted steps. Using a steady-state approach as discussed by ZB,[4] $k_{31}^{(T)}$ is given by (in our notation)

$$k_{31}^{(T)} = \left( \frac{k_{21} k_{32}}{k_{12} + k_{32}} \right) + k_{31}^{(C)}, \tag{41}$$

where the first and second term in the right-hand side repre-

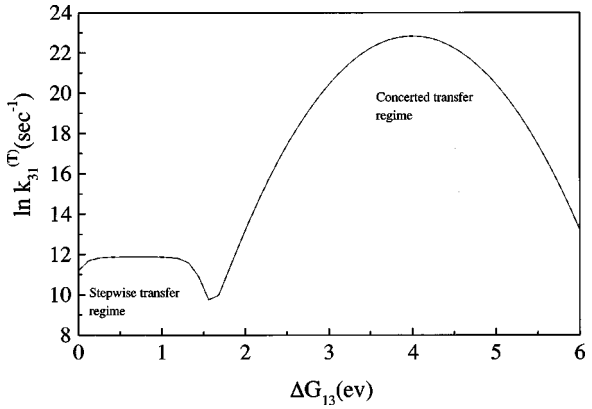


FIG. 2. Driving-force dependence of the total electron transfer rate from state 1 to state 3 in the nonadiabatic limit (when **h** matrix is set to be a unit matrix). The parameters used for the calculation are $\lambda_{12}=\lambda_{23}=1$ eV, $\lambda_{13}=4$ eV, $|V_{12}|=|V_{23}|=0.01$ eV, $|V_{13}|=0.001$ eV, and $\Delta G_{21}$ is held constant at a value of 0.3 eV.

sent sequential and concerted rates, respectively. Let us first calculate the total transfer rate in the nonadiabatic or golden rule limit by equating the **h**-matrix in Eq. (28) to a unit matrix. Following Eqs. (1) and (15), one can rewrite the expression for equilibrium population distribution given by

$$\overline{\rho}_m(x_{mn}) \propto \exp\left[-\frac{x_{mn}^2}{k_B T}\right], \tag{42}$$

so that in the nonadiabatic limit the size of the sink line, $x_{mn}$ to be used to calculate the rates is precisely determined by

$$-3\sqrt{\frac{k_B T}{2}} < x_{mn} < 3\sqrt{\frac{k_B T}{2}}. \tag{43}$$

Using this prescription, the ET rates are calculated and the results compared with those obtained from analytical expression Eq. (25) for several values of step size [that have been used to evaluate the integrals in Eq. (27)] until convergence of the results was obtained. The knowledge thus gained is subsequently utilized to obtain the converged results for solvent dynamics-influenced rates, with different range and step size for $x_{mn}$ as well as temporal step size that is used to calculate the elements of the **g**-matrix.

The free energies of reaction, the solvent reorganization energies, and the electronic coupling strengths are the input parameters needed to obtain the total transfer rates in the golden rule rate limit. Of these, the solvent reorganization energy for one-ET steps are chosen to be 1 eV; a typical value as commonly encountered in polar solvents. The electronic coupling strengths are taken to be physically reasonable such that $V_{12}, V_{23} \gg V_{13}$. With these parameters, the natural logarithm of the total transfer rate for two-ET process is presented in Fig. 2 as a function of free-energy difference between surfaces 1 and 3, while that between 1 and 2 is kept fixed to help delineate the dominance or competitiveness of stepwise and concerted rates. Plotted in this figure also is the total rate obtained from the analytical results [Eq. (25)] which overlaps with our numerical result and cannot be viewed separately in this figure. The features of this figure clearly suggest the dominance of stepwise and concerted process over each other as well as their competition, and is nicely explained by ZB.[5] In particular, in the linear portion of the curve when the total transfer rate does not change (although the driving force of transfer between surfaces 1 and 3 increases) it is suggestive of the fact that stepwise transfer dominates. Later, at a higher value of $\Delta G_{13}$, the total rate drops, indicating the effective competition between stepwise and concerted processes. As the reaction exothermiticity between surfaces 1 and 3 increases further, the usual parabolic Marcus dependence for concerted process is obtained. Thus, a variation of $\Delta G_{13}$ while keeping the $\Delta G_{21}$ value fixed elucidates the transfer mechanism at different arrangements of free-energy wells 1 and 3. The result presented in Fig. 2 in the absence of solvent effects is similar to Fig. 3 of ZB.[5]

It can be easily proved that the necessary condition for the application of Eq. (41) to obtain the total transfer rates is $k_{12}+k_{32} \gg k_{21}, k_{23}, k_{13}, k_{31}$ so that the steady-state condition pertaining to the intermediate state 2 is satisfied. This condition implies that the intermediate state $(D^+ \cdots A^-)$ is unstable and the reaction proceeds without detectable concentration of this state in the long-time limit. With increasing adiabaticity of the reaction, the rates couple to the solvent relaxation mode. And the total rate in this limit involves the one- and two-ET rates, which are in turn obtained when all three electronic states with nonzero electronic coupling between them are participating in the reaction. Thus, the sequential and concerted transfer might influence each other under suitable conditions, driven by solvent diffusion. As mentioned in the introduction, the correlation effect between the transfer in the presence of one sink with that in the presence of multiple sinks on the total rate can be seen to be fully accomplished by the use of Eq. (27), followed by Eq. (41), because in our formulation each of the three electronic states is coupled to two other sinks.

Evidently, the consideration of nonzero coupling elements along all three crossing points in the present three-surface problem is not always important. For example, as shown in Fig. 2, because of the high activation barrier for transfer from state 1 to 3, the concerted process can be neglected in the stepwise sequential transfer zone. With an increase in $\Delta G_{13}$, the crossing point between surfaces 1 and 3 shifts down and the activation barrier for the concerted process becomes smaller. Concomitant with this is the fact that the activation barrier for the stepwise transfer 2 to 3 increases. As a result, the concerted process dominates at a sufficiently high $\Delta G_{13}$ value. And when the latter approaches the activationless limit, all the population from state 1 is pumped into state 3 without any significant transfer to state 2, so that stepwise transfer $2 \rightarrow 3$ can be neglected. Therefore, when the pure stepwise or pure concerted process is controlled by solvent motion, one expects the individual transfer rates $k_{31}$ and $k_{32}$ to be zero, respectively. Instead, these individual transfer rates for pure transfer processes are found to be negative, satisfying the detailed balance condition [Eq. (17)].

Note the ET rates that we consider here are in the long-time limit. But in reality, they are time dependent. The negative transfer rates as discussed above might also be explained

by considering a time-dependent rate kernel with memory effects. In the present work, whenever we have found a negative transfer rate for that choice of input parameters and for a finite value of the Laplace parameters (such that negative rates still hold), we have calculated the Laplace transformed population, $\mathbf{P(s)}=(\mathbf{s}-\mathbf{K(s)})^{-1}$. The Laplace-transformed populations thus obtained are found to follow the relation $\Sigma^{3}_{i=1}P_{ij}(s)=1/s$ (for $j=1,2,3$) as it should be. Thus, for the present work the negative rate for a given transfer step can be thought to be rather spurious and is a simple manifestation of the fact that the transfer process is highly improbable.

Before we consider the graphical results of rate calculations in the solvent dynamics-influenced limit, it will be worthwhile to describe the criterion for choice of arrays of parameters that has been used to obtain such results. The size of electronic energy differences for one-ET reaction is characterized by the reorganization energy $\lambda$. Let us characterize the time scale of nuclear motion by an inverse of the nuclear relaxation rate, $\Lambda$, and denote the typical size of electronic coupling by $V$. Let us assume that

$$\lambda \gg \hbar\Lambda, \tag{44}$$

and

$$\lambda \gg V, \tag{45}$$

such that these inequalities comply with Eq. (2).

For typical choice of parameters, $0.1\,\mathrm{eV}\leqslant\lambda\leqslant 1\,\mathrm{eV}$ and $1.0\,\mu\mathrm{eV}\leqslant\hbar\Lambda\leqslant 10\,\mathrm{meV}$ for $0.1\,\mathrm{ps}\leqslant\Lambda^{-1}\leqslant 1\,\mathrm{ns}$, Eq. (44) can be assumed to be satisfied. Then, Eq. (45) gives an upper limit for $V$. On the other hand, to have a diffusion controlled limit, we need larger coupling strength $V$

$$\frac{V^2}{\lambda\hbar\Lambda}\gg 1, \quad \text{for } \frac{(\Delta G+\lambda)^2}{4\lambda k_{\mathrm{B}}T}\gg 1 \text{ and } \frac{(\Delta G-\lambda)^2}{4\lambda k_{\mathrm{B}}T}\gg 1, \tag{46}$$

$$\frac{V^2}{\sqrt{\lambda\hbar k_{\mathrm{B}}T\Lambda}}\gg 1, \quad \text{for } \frac{(\Delta G+\lambda)^2}{4\lambda k_{\mathrm{B}}T}\ll 1 \text{ and } \frac{(\Delta G-\lambda)^2}{4\lambda k_{\mathrm{B}}T}\ll 1. \tag{47}$$

Equations (46) and (47) are recast as

$$V\gg\sqrt{\lambda\hbar\Lambda}, \quad \text{for } \frac{(\Delta G+\lambda)^2}{4\lambda k_{\mathrm{B}}T}\gg 1 \text{ and } \frac{(\Delta G-\lambda)^2}{4\lambda k_{\mathrm{B}}T}\gg 1, \tag{48}$$

$$V\gg\sqrt{\sqrt{\lambda\hbar k_{\mathrm{B}}T\Lambda}}, \quad \text{for } \frac{(\Delta G+\lambda)^2}{4\lambda k_{\mathrm{B}}T}\ll 1 \text{ and } \frac{(\Delta G-\lambda)^2}{4\lambda k_{\mathrm{B}}T}\ll 1. \tag{49}$$

To have a diffusion-influenced limit in our system for appropriate $V$, the lower limits for $V$ given by Eqs. (48) and (49) must be smaller than the upper limit given by Eq. (45), i.e.,

$$\lambda\gg\hbar\Lambda, \quad \text{for } \frac{(\Delta G+\lambda)^2}{4\lambda k_{\mathrm{B}}T}\gg 1 \text{ and } \frac{(\Delta G-\lambda)^2}{4\lambda k_{\mathrm{B}}T}\gg 1, \tag{50}$$

$$\lambda^3\gg k_{\mathrm{B}}T(\hbar\Lambda)^2, \quad \text{for } \frac{(\Delta G+\lambda)^2}{4\lambda k_{\mathrm{B}}T}\ll 1 \text{ and } \frac{(\Delta G-\lambda)^2}{4\lambda k_{\mathrm{B}}T}\ll 1. \tag{51}$$

These two conditions always hold for $k_{\mathrm{B}}T=0.026\,\mathrm{eV}$ and for the choice of parameters as mentioned above. For the concerted process, the reorganization energy is much higher and the coupling strength is at least an order of magnitude less than that of one-ET steps. And therefore, to satisfy these two conditions the solvent relaxation rate needs to be much slower.

The normalized time-correlation function of the reaction coordinate is given by[19]

$$M(t)=\sum_{\alpha}\frac{\lambda_{\alpha,mm'}}{\lambda_{mm'}}M_{\alpha}(t), \tag{52}$$

where $M_{\alpha}(t)$ is given by Eq. (23). It had been shown before by Rasaiah and Zhu[12(c)] that this time-correlation function is equal to the time-correlation function of the Born free energy of solvation of reaction intermediates, $S(t)$, both in the continuum as well as in discrete molecular solvents provided the solvent response to the polarization field is linear. This gives an opportunity to obtain the coefficients and $\Lambda_{\alpha}$ values that appeared in Eq. (52) from experimentally determined quantities such as $S(t)$. For example, Jarzeba *et al.*[22] have measured the solvent dynamics in many solvents that can be fitted to a biexponential form given by

$$S(t)=C_1\exp(-t\Lambda_1)+C_2\exp(-t\Lambda_2), \tag{53}$$

such that $C_1+C_2=1$. One can also define an average solvation time $\Lambda_a^{-1}$ in a one-dimensional effective coordinate system given by

$$\Lambda_a^{-1}=\int_0^{\infty}S(t)dt=\frac{C_1}{\Lambda_1}+\frac{C_2}{\Lambda_2}. \tag{54}$$

### A. Pure sequential transfer

In Figs. 3–5 we present the results for pure sequential rate (when concerted rate $k_{31}^{(C)}$ is negative) for solvents like methanol, propanol, and benzonitrile, respectively. For comparison, we have also plotted in these figures the rates obtained assuming a one-dimensional effective coordinate system. Plotted in these figures also are the rates for the same solvents, assuming it to represent a Debye characteristic $[S(t)=\exp(-t\Lambda_L)]$ with a relaxation time equal to the longitudinal relaxation time, $\Lambda_L^{-1}$. For two-solvent coordinate systems (plot 1 in these figures), the coefficients and solvent relaxation time scales were obtained from Ref. 22. For one-dimensional effective coordinate systems (plot 2 in these figures), the solvation times were obtained using Eq. (54). And the longitudinal relaxation time for the same solvent (plot 3) was obtained from Ref. 14. In these figures, the other parameters are the same as in Fig. 2. In all these figures, the value of the parameter $\Delta G_{21}$ chosen also complies with the limiting assumptions used by ZB[4] in their derivation of long-time rates. It is interesting to notice in Figs. 3–5 that the sequential rate which is invariant with respect to overall driving force of the reaction in Fig. 2 (where the solvation dynamics

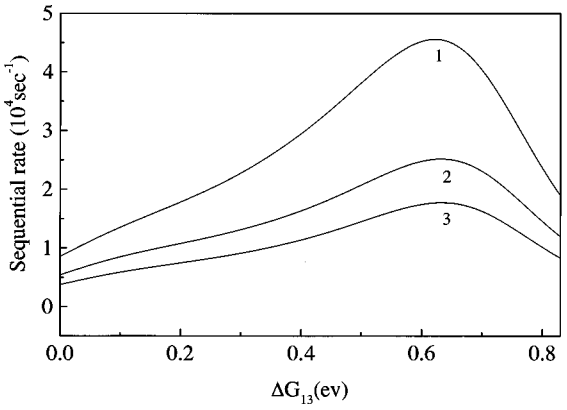


FIG. 3. Dependence of the sequential transfer rate in methanol solvent on the free-energy $\Delta G_{13}$ for a fixed value of $\Delta G_{21}$ as in Fig. 2. The electronic coupling strengths and the solvent reorganization energies are also the same as in Fig. 2. Plot 1: two solvent coordinate system such that $\Lambda_1^{-1}=1.16$ ps, $\Lambda_2^{-1}=9.57$ ps and $C_1=\lambda_{1,12}/\lambda_{12}=\lambda_{1,23}/\lambda_{23}=\lambda_{1,13}/\lambda_{13}=0.4$, $C_2=\lambda_{2,12}/\lambda_{12}=\lambda_{2,23}/\lambda_{23}=\lambda_{2,13}/\lambda_{13}=0.6$ (Ref. 22). Plot 2: Effective one-dimensional solvent coordinate system [cf. Eq. (54)] such that $\Lambda_a^{-1}=6.21$ ps and $d_{2m}=0$. Plot 3: methanol solvent with Debye characteristic with longitudinal relaxation time, $\Lambda_L^{-1}$ equal to 9.2 ps (Ref. 14).

were ignored), is now dependent on it. This can be understood as follows. With an increase in $\Delta G_{13}$ value, the reaction exothermiticity of the sequential step $2\rightarrow 3$ increases and when the final product well 3 reaches the bottom of intermediate state 2 (at $\Delta G_{13}=0.7$ eV), then this sequential step become activationless. Thus, $k_{32}$ increases as a function of $\Delta G_{13}$, and at even higher exothermiticity the Marcus-inverted regime is reached, where the activation barrier appears once again, followed by a decrease in the rate $k_{32}$. This signature of variation of $k_{32}$ vs $\Delta G_{13}$ is true both in the presence and absence of solvent dynamics effects.

However, when the solvent dynamics controls the ET rates, parallel to the increase in the rate of the transfer process $2\rightarrow 3$, $k_{21}$ (and therefore $k_{12}$) also increases, rendering the sequential rate to show a maximum value as a function of overall driving force of the reaction. Consequently, it appears that in the solvent dynamic control limit, the ET rate

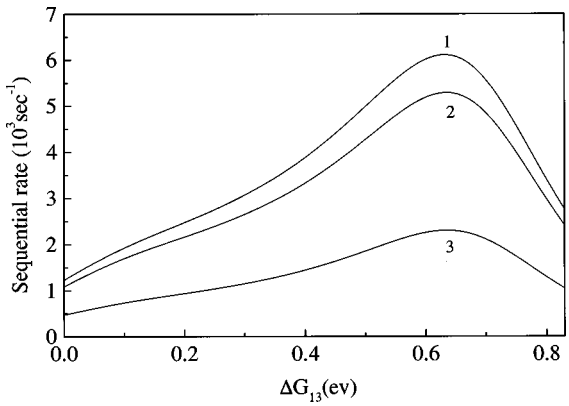


FIG. 4. Same as Fig. 3 in propanol solvent. Plot 1: two-solvent coordinate system with $\Lambda_1^{-1}=14$ ps, $\Lambda_2^{-1}=40$ ps, and $C_1=0.3$, $C_2=0.7$ (Ref. 22). Plot 2: effective one-dimensional solvent coordinate system such that $\Lambda_a^{-1}=33$ ps and $d_{2m}=0$. Plot 3: with Debye characteristic, $\Lambda_L^{-1}=77$ ps (Ref. 14).

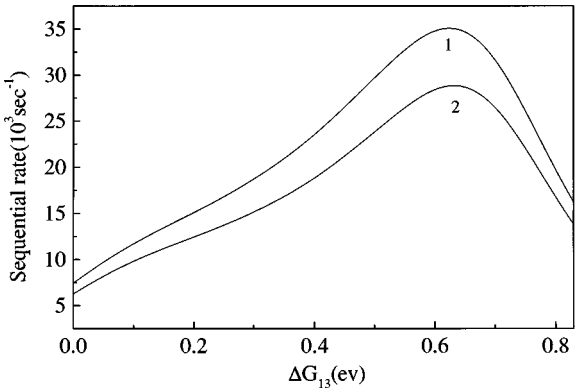


FIG. 5. Same as Fig. 3 in benzonitrile solvent. Plot 1: two-solvent coordinate system with $\Lambda_1^{-1}=2.3$ ps, $\Lambda_2^{-1}=8.2$ ps, and $C_1=0.49$, $C_2=0.51$ (Ref. 22). Plot 2: effective one-dimensional solvent coordinate system such that $\Lambda_a^{-1}=5.3$ ps and $d_{2m}=0$.

from 1 to 2 is strongly correlated with the presence of another channel of reaction from state 2. Stated qualitatively, with an increase in the rate $k_{32}$ the population of the intermediate level 2 decreases. (Note that the back transfer from more stabilized state 3 to 2 can be neglected.) Concomitant with the decrease in the population of state 2, diffusion becomes more efficient at the crossing point between surfaces 1 and 2 that drags in more population from state 1 to neutralize the population holes created in surface 2. This is reflected in the increase of the rate $k_{21}$. Thus, transfer efficiency at a given crossing point within a surface is affected by the fact that another source or sink is also present on that surface.

It is also interesting to note that such an effect is more prominent in the case of non-Debye solvents with two characteristic relaxation time scales than that in the case of solvent with a single relaxation time scale. This enhancement of the transfer rates in non-Debye solvents is not unusual. For example, in Ref. 12(c) Rasaiah and Zhu have found that the survival probabilities of the reactants undergoing ET reactions depend on the nature of time correlation of the reaction coordinate used. A biexponential form of the correlation function gives rise to a faster decay of the reactant survival probabilities when compared to an effective single-exponential time dependence of the same correlation function. Results of single solvent coordinate systems presented in Figs. 3–5 are obtained by setting $d_{2m}$ equal to zero such that the curve-crossing manifolds of potential surfaces reduce to a single intersection point. With the use of a two collective solvent coordinate, the presence of multiple sinks is obvious (cf. Fig. 1). Thus, the presence of an extra dimension in our formalism can be thought to open up a new channel for reaction and the impact of this on the long-time rates is quite significant, as is evident in these figures (compare plot 2 with plot 1). On the other hand, use of a single solvent coordinate with characteristic relaxation time equal to the longitudinal relaxation time gives the lowest estimates of the rates. Longitudinal relaxation time of a solvent is indeed a bulk property of the solvent. In contrast, the empirically determined average solvation times of these solvents is microscopic in nature and gives rise to higher estimates of

rates, closer to the values obtained using a more microscopic two-dimensional solvent coordinate model.

If one employs the generalized Langevin equation formalism to obtain reaction coordinate dynamics, then solvent relaxation time scales along these coordinates can be thought to represent the measure of the time-dependent friction kernel. The latter quantity characterizes dissipation effects of the solvent motion along the reaction coordinate. The less the solvent relaxation time, the less the friction. For a two-solvent coordinate system, the second dimension offers a bypass for the diffusional flux of the reactants to approach the sink line, even when the frictional resistance along the other dimension might be relatively larger. In view of this, the reason that the highest rate is calculated for methanol followed by benzonitrile and propanol solvent directly follows from a comparison of the time scales of relaxation along the two coordinates for these solvents. Note that the rates presented in Figs. 3–5 are experimentally observable rates which happen to be pure sequential transfer rates. When the sequential and concerted transfer processes are competitive, the composite of these two is observable, which we will discuss shortly.

### B. Pure concerted transfer

When the overall reaction exothermiticity becomes sufficiently high such that the intermediate state can be ignored, then a pure concerted transfer mechanism prevails. Apart from the fact that in the concerted process of transfer, two electrons are transferred in a single step with its associated high solvent reorganization energy, the dynamical solvent control of such a process can be thought to be equivalent to single electron transfer reaction.[8–16,19] Once again, the concerted ET rates calculated in a two-dimensional solvent system (for arbitrarily chosen solvent with an equal weighting of relaxation dynamics along the two coordinates) were found to be higher when compared with the corresponding average and effective solvent coordinate system.

For further discussion, let us denote the crossing points between donor–acceptor states 1 and 2 by $c_{12}$, between 2 and 3 by $c_{23}$, and that between 1 and 3 by $c_{13}$. When the cross point $c_{13}$ lies far apart from the other two crossing points, the ZB strategy of separate evaluation of stepwise and concerted rates is a reasonably good approximation. But, when the three cross points are closely located (cf. Fig. 2, the region around where the total rate first drops down and then increases), this assumption becomes questionable. Because in that case, reaction in different channels might interfere with each other. This interference arises solely from solvent diffusion effects and can lead to a new solvent dynamic effect being observed, caused by nonequilibrium sequential transfer of the nuclear wave packet. The more specific physical conditions needed to obtain such effects are elaborated elsewhere.[21]

### C. Competing sequential and concerted transfer

To understand the interference of reaction channels, let us first consider the effects of variation of electronic coupling strengths on the ET rates in methanol solvent. This is

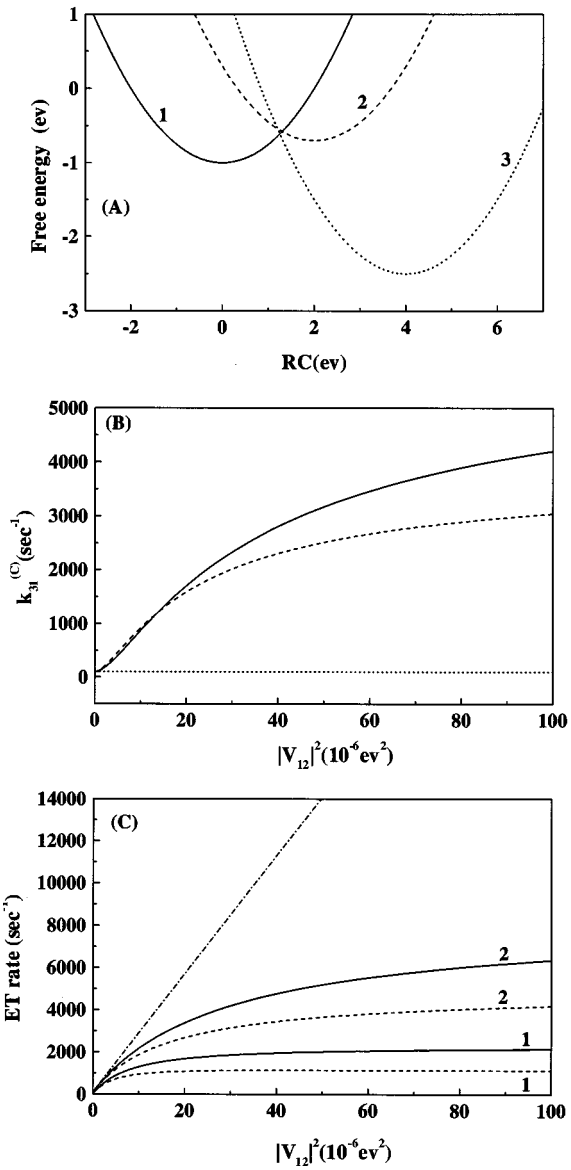


FIG. 6. (A) Free energies of the three surfaces (1, 2, and 3) of a polarization field as a function of reaction coordinate for $\Delta G_{21}=0.3$ eV and $\Delta G_{13}=1.5$ eV. $\lambda_{mm'}$ are same as in Fig. 2. (B) Concerted ET rate for the same free-energy relationship plotted as a function of electronic factor $|V_{12}|^2$ ($|V_{12}|=|V_{23}|$ and $|V_{13}|^2=4\times10^{-8}$ eV$^2$) in methanol solvent with the same solvent parameters as in Fig. 3. Solid and dashed lines represent two- and effective one-dimensional solvent coordinate system, respectively. Dotted line: Intrinsic nonadiabatic rate. (C) Corresponding total (marked as 2) and sequential (marked as 1) rate. Solid and dashed lines have similar meaning as in Fig. 6(B). The dashed dotted line is the nonadiabatic counterpart of total ET rate.

illustrated in Figs. 6 and 7. For convenience, the free energies (of the three surfaces) of a polarization field as a function of reaction coordinate is also shown in these figures. $\Delta G_{21}$ is once again taken to be equal to 0.3 eV. In Fig. 6, $\Delta G_{13}=1.5$ eV and $V_{13}$ is kept fixed at a value of $2\times10^{-4}$ eV, while in Fig. 7 $\Delta G_{13}=1.9$ eV and $V_{12}=V_{13}=0.01$ eV. In both of these figures, the solvent reorganization energies are the same as in Fig. 2.

As can be seen in Fig. 6(A), the three intersection points between the free-energy surfaces are almost overlapping with each other. It is well known that the intrinsic rate of

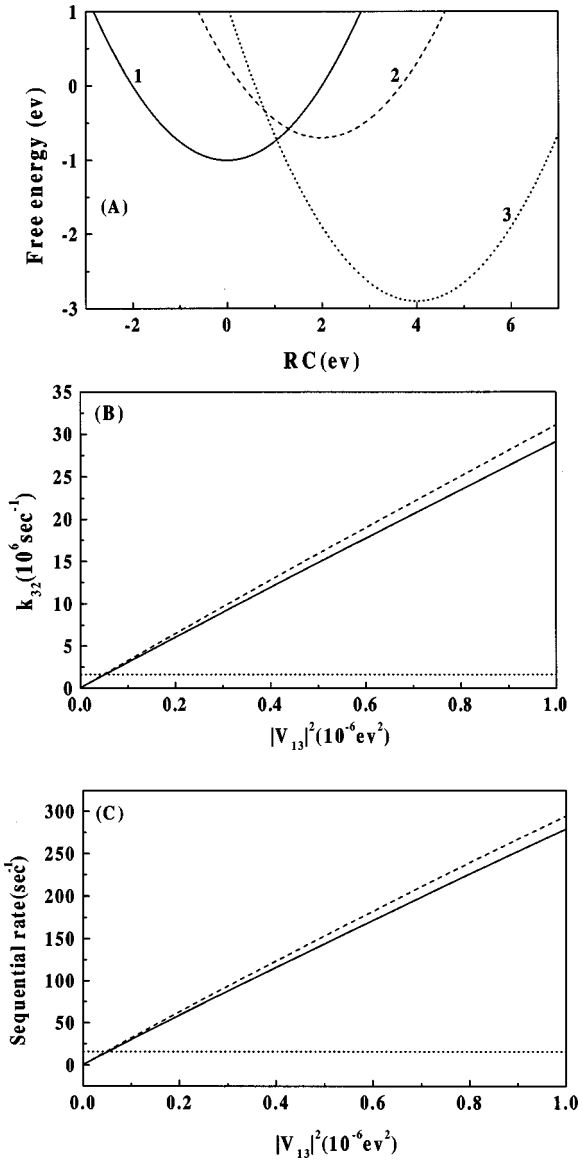


FIG. 7. (A) Same as Fig. 6(A) but for $\Delta G_{13}=1.9$ eV. (B) Transfer rate $k_{32}$ for the same free-energy relationship vs $|V_{13}|^2$ ($|V_{12}|=|V_{23}|=0.01$ eV) in methanol solvent with the same solvent parameter as in Fig. 3. Solid, dashed, and dotted lines have similar meaning as in Fig. 6(B). (C) Corresponding sequential transfer rate. Solid and dashed lines have similar meaning as in Fig. 6(B), while the dotted line represents nonadiabatic counterpart of sequential rate.

reaction $1\rightarrow 3$ is given by the nonadiabatic rate constant with coupling $V_{13}$ functioning at the crossing point $c_{13}$. Therefore, the concerted nonadiabatic rate, shown by the dotted line in Fig. 6(B) [obtained by equating the **h**-matrix to a unit matrix in Eq. (27)], will be independent of the variation of coupling strengths between 1 and 2 or between 2 and 3. It is also well known that in the presence of a solvent dynamic effect, the $1\rightarrow 3$ (assuming that the intermediate state is absent) transfer step will give rise to rates lower than its nonadiabatic counterpart. However, it is interesting to note that when the dynamical solvent effect couples the three transfer kinetics along the three intersection points (such that the **h**-matrix differs from being a unit matrix), the rate $k_{31}^{(C)}$ does depend on the variation of coupling strengths at $c_{12}$ and $c_{23}$, and is much higher than its nonadiabatic counterpart.

This enhancement of the concerted rate $k_{31}^{(C)}$ over its nonadiabatic limit is a direct manifestation of the interference of the second intermediate state that couples with the transfer process between 1 and 3 through the dynamic solvent effect. This can be justified as follows. Before the reaction starts, the equilibrium position of the population wave packet is peaked at the bottom of the free-energy surface 1 [cf. Fig. 6(A)]. As the reaction proceeds, the population wave packet crosses the intersection point $c_{13}$ that gives rise to usual long-time concerted rates. The population wave packets created at the crossing point $c_{12}$ will first stabilize through solvent polarization in surface 2, where it undergoes the usual transfer to state 3, giving rise to the sequential transfer $2\rightarrow 3$. However, in the process of stabilization on surface 2, the width of the population wave packets created at $c_{12}$ increases with respect to time due to overdamped diffusion and the moment it becomes greater than the distance between crossing points $c_{12}$ and $c_{23}$; a non-negligible population of $(D^+\cdots A^-)$ will leak through the cross point $c_{23}$ before being thermally equilibrated at surface 2. This additional contribution to the concerted rate, which has been termed nonequilibrium sequential transfer in Ref. 21, will of course be a function of coupling strengths $V_{12}$ and $V_{13}$. And therefore, the concerted ET rate dependence on the coupling strength $V_{12}$ can be seen to be of similar nature as the stepwise ET rate [compare Fig. 6(B) with 6(C)]. It is interesting to note that leakage of population (and therefore the ET rate) through this mechanism is more important for the methanol solvent with two collective coordinates than that when it is represented by an effective one-coordinate system. The total concerted rate from surface 1 to 3 is not simply a sum of two contributions arising from two separate channels ($1\rightarrow 3$, and $1\rightarrow 2$, and then $2\rightarrow 3$ before a thermal equilibration is attained at state 2), and cannot be considered separately. Rather, the ET rate matrix elements given by Eq. (27) are adequate to take into their joint influence the rate $k_{31}^{(C)}$.

Figure 6(C) shows the various ET rates vs coupling strengths between surface 1 with 2. Evidently, the observable total ET rate is significantly higher than that of the sequential rate, more so for a solvent with two collective coordinates. Clearly, the separate evolution of the sequential rate (such that $V_{13}=0$) and the concerted rate (such that surface 2 is absent) and later adding them to obtain the total observable rate from 1 to 3 will be erroneous. In that case, the interference of reaction channels as described above will be ignored.

We now turn to another example of interference of reaction channels as a function of coupling strength $V_{13}$, as illustrated in Fig. 7. The free-energy profile in Fig. 7(A) suggests a concerted mechanism will dominate over the sequential transfer steps. However, as shown in Figs. 7(B) and 7(C), the influence of the electronic factor $V_{13}$ on the sequential ET rate is enormous compared to that when the solvent dynamic effects are assumed to be absent. Also, it can be observed in this figure that such an effect is slightly larger for solvents with effective one-dimensional diffusion coordinates. The reason for such behavior can be justified as follows. The ion pair state $(D^+\cdots A^-)$ from its equilibrium position at surface 2 can undergo two transitions, one at crossing point $c_{12}$, which is responsible for reverse transfer,

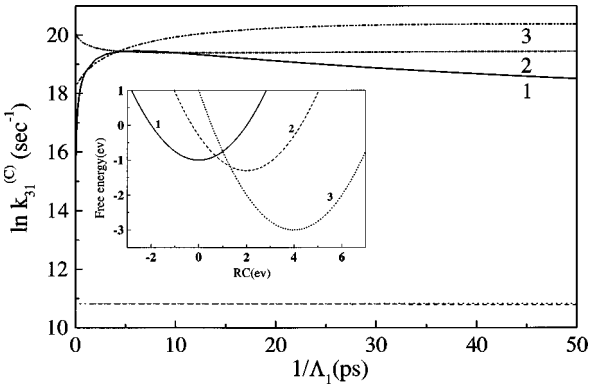


FIG. 8. The natural logarithm of the concerted rate plotted as a function of solvent relaxation time. $\Delta G_{21}=-0.3$ eV, $\Delta G_{13}=2$ eV, $|V_{12}|=|V_{23}|=3\times10^{-3}$ eV, $|V_{13}|=3\times10^{-4}$ eV, and solvent reorganization energies are same as in Fig. 2. Lines marked with numbers are for the situation when all three surfaces are taking part in the reaction with various representations of the solvent polarization; 1: one-dimensional ($d_{2m}=0$, $m=1,2,3$), 2: two-dimensional with $\Lambda_2^{-1}=10$ ps, 3: two-dimensional with $\Lambda_2^{-1}=1$ ps. Dashed line: when second intermediate surface is absent. Dotted line: nonadiabatic transfer rate. Inset shows the free energies of the three surfaces of a polarization field.

and the other at $c_{23}$, which is responsible for the usual transfer $2\rightarrow3$. The latter rate represented by the dotted line in Fig. 7(B) clearly shows that such intrinsic transfer rate in the absence of solvent dynamics is independent of the coupling factor $V_{13}$. However, in the presence of a dynamical solvent effect as the $(D\cdots A)$ population created at $c_{12}$ (due to back transfer from state 2) relaxes down to the minimum of free-energy surface 1, will experience the cross point $c_{13}$. And, a large fraction of population will move to surface 3 before being thermally equilibrated at surface 1. This additional transfer of population to surface 3 adds to the higher rate of transfer $k_{32}$ and eventually becomes a function of coupling factor $V_{13}$. As such a mechanism is solvent dynamics-dependent, the dashed and solid lines in Figs. 7(B) and 7(C) are only germane for comparison purposes. Namely, in a solvent with two collective coordinates with one of its relaxation time scales much faster than what the solvent could be represented by, an effective one-dimensional diffusion, the $(D\cdots A)$ population created at $c_{12}$ will relax to the equilibrium at the minimum of surface 1 much quicker, rendering the rate $k_{32}$ less as compared to the effective one-coordinate case.

Concomitant with the increase in $k_{32}$ as a function of $V_{13}^2$, the one-ET rate $k_{12}$ decreases (not shown in the figure). This variation might offer a possibility to verify the predictions of this work by electrochemical method when the transfer channels are competing with each other. For example, a kinetic discrimination between one-ET rates of a two-ET reaction by electrochemical method[2(b)] is possible if the one-ET rates considerably differ from one another such that a variation in voltametric sweep rate can clearly distinguish between the two-electron waves.

In order to further delineate the new solvent dynamic effect that couples the internal dynamics of the three free-energy surfaces, we have presented in Fig. 8 the concerted rate, $k_{31}^{(C)}$ as a function of solvent relaxation time. The parameters chosen are $\Delta G_{13}=0.2$ eV; electronic coupling strengths and solvent reorganization energies are the same as in Fig. 2. Unlike previous figures, $\Delta G_{21}$ is taken to be equal to $-0.3$ eV, i.e., the reaction is thought to proceed through a stable intermediate. However, the presence of a more stable final product state 3 guarantees the fact that $k_{12}+k_{32}\gg k_{21},k_{13},k_{31}$ such that the steady-state condition to the population in state 2 can be applied to obtain the total rate as given in Eq. (41). The inset in Fig. 8 shows the free energy of polarization in a one-dimensional coordinate system as obtained from utilizing Eq. (33). Plotted in the figure are the ET rates obtained using a one-solvent coordinate system and those obtained using a two-solvent coordinate system with the coefficients in Eq. (53) taken to be 0.5 when the relaxation time along the second coordinate is kept fixed. For the sake of comparison, also plotted in this figure are the nonadiabatic intrinsic transfer rate from 1 to 3 and the transfer rate in the presence of solvent dynamic effects when the second diabatic surface is absent. The last mentioned ET rate corresponds to the purely concerted process when $V_{12}=V_{23}=0$. Since the activation energy for such a process is rather high and the $V_{13}$ coupling element is small, as expected a pure concerted rate under such a situation will only be weakly solvent-dynamic dependent. However, when all three surfaces are participating in the transfer reaction (compare with the lines marked with numbers in Fig. 8), the solvent dynamics effects give rise to a much higher rate of transfer as compared to its nonadiabatic counterpart.

As can be seen in Fig. 8, when the solvent with a Debye characteristic couples with the internal dynamics between the three surfaces, the ET rate increases as the solvent relaxation time decreases until around 6 ps, when the transfer rate is maximum, and finally the ET rate decreases to equate to its nonadiabatic limit when the solvent relaxation time is close to 0 ps. This behavior can be conceptualized as follows. The ion pair state $(D^+\cdots A^-)$ produced at the crossing point $c_{12}$ relaxes downward along the surface 2 to attain the thermal equilibrium. In the process of relaxation driven by diffusion, the population wave packet experiences another crossing point $c_{23}$, where one more electron is transferred to produce the final product before the former wave packets can finally relax into state 2. This additional ''hot ion pair'' population contributes toward the higher concerted rate. Since the process of such transfer is diffusion driven, it is likely only that the ET rate arising from such effects will be solvent-dynamic dependent, as is evident in this figure. In a Debye solvent with sufficiently fast relaxation time ($<6$ ps), much faster than the transfer time, the ion pair produced at cross point $c_{12}$ will quickly attain the thermal equilibrium in surface 2 rather than transferring one more electron at $c_{23}$. Consequently, the contribution to the rate from nonequilibrium population at surface 2 decreases. This causes the concerted rate to decrease until it attains the nonadiabatic limit at around 0 ps. This can also be confirmed by comparison with the same ET rate in solvents with two-characteristic relaxation time. In the case of a solvent with two collective coordinates, where the reaction is thought to take place along a line of sink density, the presence of a second relaxation coordinate will certainly give rise to a higher rate, as long as

the overall impact of relaxation dynamics along the two solvent coordinates on the transfer rate is sufficiently slow to prevent quicker equilibration at surface 2 (so that the nonequilibrium population contribution to the rate is significant). For the arbitrary solvent chosen to construct Fig. 8, when $\Lambda_2^{-1}$ is held fixed at 1 ps and the other coordinate also represents fast relaxation, the rate decreases sharply following a quicker equilibration of population wave packets at surface 2. On the contrary, when $\Lambda_2^{-1}$ is taken to be 10 ps, the response from this coordinate remains too sluggish to show the same behavior, even though the other coordinate represents fast relaxation and is close to 0 ps.

## IV. CONCLUSION

In short, we have developed in this work a theoretical recipe to calculate long-time multiple ET rates in solvents with multiple relaxation time scales. However, we have presented some example calculations for two-ET reactions in view of their immense importance in the electrochemical and biological redox processes (to name a couple). The theoretical method depends on the choice of nuclear collective coordinates[19] that directly follows from solvent spectral densities or from the experimentally determined time-correlation function $S(t)$ for the free energy of solvation of reactants. When the influence of the solvent can be represented as a single overdamped coordinate, the potential energy curve-crossing manifold as depicted in Fig. 1 reduces to a single point and the system can be thought to represent a Debye solvent. This is the situation considered by ZB[4,5] apart from its several limiting assumptions. Our example calculations clearly manifest the effects of considering a curve-crossing manifold rather than a single crossing point on the potential energy surfaces. In this work, we have also presented the criterion for the choice of reorganization energies, solvent relaxation rates, and electronic coupling factor that can give rise to solvent dynamics-influenced transfer rates.

The restriction on the separate evolution of stepwise sequential ($V_{13}=0$) and concerted ($V_{12}=V_{23}=0$) ET rates are illustrated especially in the regime where the intersection points among the three free-energy surfaces lie close to each other. In such situations, as illustrated in this work, the diffusion-driven hot ion pair population contribution to the observable stepwise or concerted rate can, interestingly, become a nonlinear function of coupling strengths such as $V_{13}$ or $V_{12}$, respectively. According to the present formalism for purely stepwise or concerted processes, (when the crossing points lie far apart from each other), one of the long-time ET rates might become negative. Qualitatively, it simply means that such transfer processes are highly improbable and therefore can be neglected. However, in a quantitative sense this observation deserves separate attention, and a time-dependent solution of the transfer kinetics with a memory effect might resolve these subtleties.

The new solvent dynamic effect caused by the nonequilibrium sequential transfer of population wave packet, predicted in this work (cf. Figs. 6–8) can also be verified experimentally. For example, the increasing rate $k_{32}$ and what follows the decrement of the rate $k_{21}$ as a function of coupling strength $V_{13}$ might provide a suitable criterion for the ready observation of kinetic discrimination of one-ET steps in the case of electrochemical cyclic voltametry measurements.[2(b)] Similarly, the higher concerted rates compared to its nonadiabatic counterpart, presented in Figs. 6 and 8, can again be measured by the same electrochemical experiments that shows a single $2e^-$ wave with Nernstian behavior. Note that the present theoretical recipe is applicable for any arrangements of free-energy wells. This in turn suggests that the solvent dynamics effect predicted in this work, in the competitive transfer regime, can be tested and verified for a wider class of commonly used donor–acceptor pairs. In view of the recent advances[2(c)] in the photon-induced multiple ET processes in group-8-platinum cyano-bridged complexes, the possibilities of carrying out ultrafast time-resolved studies on these systems might not be far off. In this regard, the present work needs to be generalized to include an initial nonequilibrium population of the reactants.

## ACKNOWLEDGMENTS

This research was supported by Japan Science and Technology Corporation, and Center of Excellence Development Project (COE Project) on Photoreaction Control and Photofunctional Materials (PCPM). We are very thankful to Dr. K. Seki for fruitful discussions.

[1] (a) D. J. Lowe, K. Fisher, R. N. F. Thomeley, S. Vaughn, and B. K. Burgess, Biochemistry **28**, 8460 (1989); (b) J. L. Marshall, S. R. Stobart, and H. B. Gray, J. Am. Chem. Soc. **106**, 3027 (1984); (c) S. Kuwabata, K. Tanaka, and T. Tanaka, Inorg. Chem. **25**, 1691 (1986); (d) A. Ahlberg, O. Hammerich, and V. D. Parker, J. Am. Chem. Soc. **105**, 844 (1983); (e) Adam Heller, Acc. Chem. Res. **14**, 154 (1981); (f) J. P. Collin, and J. P. Sauvage, Coord. Chem. Rev. **93**, 245 (1989).
[2] (a) R. Traber, H. E. A. Kramer, and P. Hemmerich, Pure Appl. Chem. **54**, 1651 (1982); (b) D. T. Pierce and W. E. Geiger, J. Am. Chem. Soc. **114**, 6063 (1992); (c) Y. Wu, B. W. Pfennig, S. L. Sharp, D. R. Ludwig, C. J. Warren, E. P. Vicenzi, and A. B. Bocarsly, Coord. Chem. Rev. **159**, 245 (1997); (d) G. Jones, II, N. Mouli, W. A. Haney, and W. R. Bergmark, J. Am. Chem. Soc. **119**, 8788 (1997); (e) M. S. Mondal, H. A. Fuller, and F. A. Armstrong, *ibid.* **118**, 263 (1996); (f) M. Szwarc, Acta Chem. Scand. **51**, 529 (1997); (g) S. Bhattacharya, M. Ali, S. Gangopadhyay, and P. Banerjee, J. Chem. Soc. Dalton Trans. **13**, 2645 (1996); (h) S. Michael, Acta Chem. Scand. **51**, 529 (1997).
[3] M. A. Vorotyntsev and A. M. Kuznetsov, Sov. Electrochem. **6**, 196 (1970).
[4] L. D. Zusman and D. N. Beratan, J. Chem. Phys. **105**, 165 (1996).
[5] L. D. Zusman and D. N. Beratan, J. Phys. Chem. **101**, 4136 (1997).
[6] R. A. Marcus, Annu. Rev. Phys. Chem. **15**, 155 (1964).
[7] V. G. Levich, in *Physical Chemistry-An Advanced Treatise*, edited by H. Henderson and W. Yost (Academic, New York, 1970).
[8] (a) L. D. Zusman, Chem. Phys. **49**, 295 (1980); (b) *ibid.* **112**, 53 (1987); (c) *ibid.* **119**, 51 (1988).
[9] (a) D. F. Calef and P. G. Wolynes, J. Phys. Chem. **87**, 3387 (1983); (b) *ibid.* **78**, 470 (1983).
[10] (a) J. T. Hynes, J. Phys. Chem. **90**, 3701 (1986); (b) Annu. Rev. Phys. Chem. **36**, 573 (1985).
[11] (a) I. Rips and J. Jortner, J. Chem. Phys. **87**, 2090 (1987); (b) Chem. Phys. Lett. **133**, 411 (1987); (c) J. Chem. Phys. **88**, 818 (1988).
[12] (a) J. Zhu and J. C. Rasaiah, J. Chem. Phys. **95**, 3325 (1991); (b) *ibid.* **96**, 1435 (1992); (c) *ibid.* **98**, 1213 (1993); (d) T. Fonseca, *ibid.* **91**, 2869 (1989).
[13] (a) M. Sparpaglione and S. Mukamel, J. Phys. Chem. **91**, 3938 (1987); (b) J. Chem. Phys. **88**, 3263 (1988).
[14] M. Maroncelli, J. McInnis, and G. R. Fleming, Science **243**, 1674 (1989).
[15] H. Sumi and R. A. Marcus, J. Chem. Phys. **84**, 4894 (1986).
[16] (a) S. Roy and B. Bagchi, J. Chem. Phys. **100**, 8802 (1994); (b) P. F. Barbara, T. J. Meyer, and M. A. Ratner, J. Phys. Chem. **100**, 13148

(1996); (c) J. Najbar and W. Jarzeba, Chem. Phys. Lett. **196**, 504 (1992).
[17] M. Tachiya, J. Phys. Chem. **97**, 5911 (1993).
[18] T. Bandyopadhyay, A. Okada, and M. Tachiya (unpublished).
[19] A. Okada, V. Chernyak, and S. Mukamel, Adv. Chem. Phys. edited by J. Jortner and M. Bixon (Wiley, New York, 1999) Vol. 106, Pt. one.
[20] (a) E. Akesson, A. E. Johnson, N. E. Levinger, G. C. Walker, T. P. DuBruil, and P. F. Barbara, J. Chem. Phys. **96**, 7859 (1992); (b) H. Kandori, K. Kemnitz, and K. Yoshihara, J. Phys. Chem. **96**, 8042 (1992); (c) T. Kobayashi, Y. Takagi, H. Kandori, K. Kemnitz, and K. Yoshihara, Chem. Phys. Lett. **180**, 416 (1991).
[21] A. Okada, T. Bandyopadhyay, and M. Tachiya, J. Chem. Phys. **110**, 3509 (1999).
[22] W. Jarzeba, G. C. Walker, A. E. Johnson, and P. F. Barbara, Chem. Phys. **152**, 57 (1991).